# Journal of Applied Sciences

ISSN 1812-5654

science alert

ANSInet
an open access publisher
http://ansinet.com

Journal of Applied Sciences 12 (11): 1086-1092, 2012
ISSN 1812-5654 / DOI: 10.3923/jas.2012.1086.1092


# A Single Particle Growth Model in Styrene Coordination Polymerization

S.R. Sulttan, W.J.N. Fernando and Suhairi A. Sata
School of Chemical Engineering, University Sains Malaysia 14300, Penang, Malaysia

**Abstract:** In the present study, a single particle growth model is developed to study the effects of initial catalyst size and initial catalyst active site concentration on the rate of polymerization and Molecular Weight Distribution (MWD) for styrene coordination polymerization over soluble metallocene catalyst. To describe the spatial-time evolution of monomer concentration profiles in growing particles, the Polymeric Multigrain Model (PMGM) is utilized. The PMGM is solved together with kinetic scheme to predict the rate of polymerization and MWD. The model simulation showed the presence of a significant distribution of monomer concentration across the radius of particles growth. It was further noticed that, the polymerization rate increase with increasing initial active metal concentration, while changing in the opposite direction under the influence of initial catalyst size. Additionally, the MWD increase with increasing initial active metal concentration and initial catalyst size.

**Key words:** Polymeric multigrain model, particle growth, polystyrene, coordination polymerization

## INTRODUCTION

Syndiotactic Polystyrene (SPS) is a semi crystalline thermoplastic polymer with many advantageous properties such as excellent heat resistance with a high melting point of 270-272°C, strong chemical resistance against acids, bases, oils and water and low dielectric constant. The relatively fast crystallization rate makes SPS a promising material for a large number of applications in the automotive, electrical and packaging industries, (Schellenberg, 2009). The SPS was firstly synthesized in 1985 by Idemitsu Kosan Co. Ltd. (Tokyo, Japan). using a soluble titanocene compound, activated by Methylalumoxane (MAO).

The simplest description of particle growth phenomenon in polymerization reactor is based on a spherical layer of polymer particle that is formed around the spherical catalyst particle. Models based on this geometry are commonly called Solid Core Models (SCM). Monomer diffusion from the polymer shell to the active site on the catalyst surface is the central theme of these models.

The Polymeric Flow Model (PFM) was proposed by Singh and Merrill (1971) and Galvan and Tirrell (1986), this model supposes that the catalyst fragments and polymer chains grow form a continuum. Their supposition represents a big improvement in comparison to the previous models; for they do not agree with a large number of experiments in that they do not take into consideration the catalyst particle fragmentation.

Numerous of papers have been published on the polymer particle growth modelling and morphology. However, most of these studies were based on the Multi Grain Model (MGM) of Floyd *et al.* (1986a). In accordance with the numerous experiments, the MGM assumes a rapid breakup of the catalyst particles into small fragments which are distributed throughout the polymer particles. Thus, the large polymer particle (macro particles) will consist of many small molecules (micro particles) which encapsulate these catalyst fragments. For the monomer particles to reach the active sites, it must first be diffused through the pores of macro particles, between the micro particles and then to micro particles themselves. In general, the diffusion resistances in both cases are not equal; besides, they include the possibility of having an equilibrium sorption of monomer particles at the surface of micro particle.

Sarkar and Gupta (1991, 1992), derived a model called the polymeric multigrain model (PMGM) that combines features of the MGM with some features of the simplified PFM. The authors considered the early fragmentation of catalyst particles and assumed that catalyst subparticles move radially outwards in time, in proportion to the growth of polymer around them.

The models above were derived for conventional Ziegler-Natta catalysts and only a complete fragmented particle is considered, while a few models specially derived for metallocene catalysts may be found in the literature.

Bonini *et al.* (1995), showed that the MGM cannot fit experimental data involving gradual particle fragmentation

**Corresponding Author:** S.R. Sulttan, School of Chemical Engineering, University Sains Malaysia 14300, Penang, Malaysia

and developed a Particle Growth Model (PGM) for silica supported metallocene catalysts; it is based on the same ideas of the MGM but assumes a gradual fragmentation of the particle. In this way the pellet is divided into two parts: a fragmented (that behaves exactly like in the multigrain model) and an unfragmented one.

Alexiadis *et al.* (2004) derived a more general model from the Bonini *et al.* (1995), but with the addition of a further part regarding the unfragmented core for the olefin homopolymerization with metallocene catalysts.

In this study, a detail particle growth model for styrene homopolymerization over soluble metallocene catalyst, based on a combination features of the PMGM of Sarkar and Gupta (1992) and PGM of Bonini *et al.* (1995). The model considered the gradual fragmentation of catalyst particles and assumed that catalyst subparticles move radially outwards in time, in proportion to the growth of polymer around them. In addition the model is coupled with kinetics scheme to predict the polymerization rate and (MWD) of syndiotactic polystyrene at different catalyst size and active site concentration.

## MODEL DESCRIPTION

The radial gradient in the growth of polymer particles gives with the passage of time a distribution system for monomer concentration as a function of position and time. Thus, it is possible to get the physical properties of the polymer as a function of position and time.

In the present study, the PMGM was applied to simulate the single particle growth model. Just as in the PMGM, the growing polymer particle (from the soluble catalyst) is divided into shells. These shells are activated gradually from the external surface of the particle to its center, as proposed by Bonini *et al.* (1995), as shown in Fig. 1. The main difference is that the initial particle is split in two shells only, so as to take into account that our initial catalyst-particle is of molecular size.

In PMGM, the early fragmentation of catalyst particles was considered and assumed the catalyst subparticles move radially outwards in time, in proportion to the growth of polymer around them as shown in Fig. 1. In addition, it is assumed that the catalyst subparticles exist in close packed layers within a macroparticle just after fragmentation at t = 0. The number, ($N_i$) of subparticle in the ith shell at time = 0 is calculated using the radius of the individual subparticle, ($R_{c,i}$) in that shell and the void fraction ($\varepsilon = 0.4$), associated with close packed spheres. This gives Eq. a and b in Table 1.

Thus, this model incorporates a shell-wise distribution of catalyst subparticles, somewhat akin to distribution of microparticles in the PMGM and considered the gradual fragmentation of catalyst. At a later time, however, the catalyst subparticles are distributed in a continuum of polymer (Fig. 2). It is assumed that their number, ($N_i$), in any shell remains unchanged as polymerization progresses. One can follow the expansion and movement of each of the catalyst sub particles and their associated polymer from time t = 0.

To predict the spatial-temporal monomer concentrations profiles in a growing particle, the following system of dynamic molar species equations needs to be solved numerically.

$$\frac{\partial M(r,t)}{\partial t} = \frac{D_e}{r^2}\frac{\partial}{\partial r}\left(r^2\frac{\partial M}{\partial r}\right) - R_p \quad (1)$$

$$\text{I.C.} \quad M(r,0) = M_b \quad (2)$$

$$\text{B.C.1} \quad \frac{\partial M(0,t)}{\partial t} = 0 \quad (3)$$

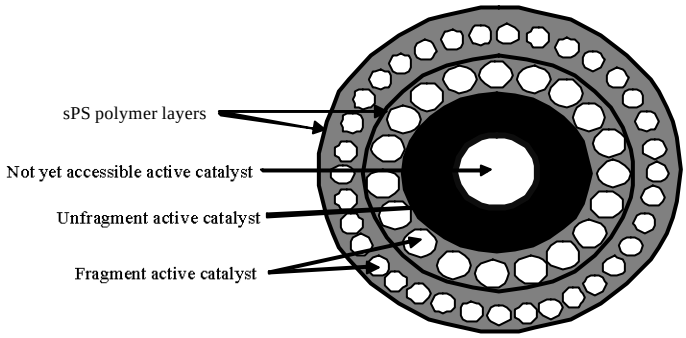


Fig. 1: Schematic representation of the SPS particle growth based on PMGM

Table 1: Equation for $N_i$ and $M_i$ for the PMGM

$$N_1 = 1 \quad (a)$$

$$N_i = \frac{6(1-\varepsilon)\left[R_{c,1} + 2\sum_{j=2}^{i-1} R_{c,j} + R_{c,i}\right]^2}{R_{c,i}^2} \qquad i=2,3,.....,N \quad (b)$$

$$M_i = M_1 \quad (c)$$

$$\frac{dM_1}{dt} \frac{2D_{e,1}(M_2 - M_1)}{(\Delta r_1)^2} - R_{p,1} \quad (d)$$

$$\frac{dM_i}{dt} = \frac{2D_{e,i}}{\Delta r_i + \Delta r_{i-1}}\left[M_{i+1}\left(\frac{1}{\Delta r_i} + \frac{1}{R_i}\right) - M_i\left(\frac{1}{\Delta r_i} + \frac{1}{\Delta r_{i-1}}\right) + M_{i-1}\left(\frac{1}{\Delta r_{i-1}} + \frac{1}{R_i}\right)\right] - R_{pi} \quad i = 2,3,.....,N+1 \quad (e)$$

$$\frac{dM_{N+2}}{dt} = -M_{N+2}\left[\frac{2k_1}{\Delta r_{N+1}} + \frac{2D_{e,N+2}}{(\Delta r_{N+1})^2} + \frac{2k_1}{R_{N+2}}\right] + M_{N+1}\left[\frac{2D_{e,N+2}}{(\Delta r_{N+1})^2}\right] + M_b\left[\frac{2k_1}{\Delta r_{N+1}} + \frac{2k_1}{R_{N+2}}\right] - R_{p,N+2} \quad (f)$$

Where:

$$R_{p,1} = R_{p,N+2} = 0 \quad (g)$$

$$R_{p,i} = \frac{(4\pi)(3600)k_p C^* M_i N_i (R_{e,i-1})^3}{\left(\frac{4\pi}{3}\right)(R_{h,i}^3 - R_{h,i-1}^3)}; \quad i = 2,3,.....,N+1 \quad (h)$$

$$D_{e,1} = D_{e,N+2} = D_1 \quad (i)$$

$$D_{e,i} = \frac{D_1 N_i R_{c,i}^3}{(R_{h,i}^3 - R_{h,i-1}^3)}; \quad i = 2,3,.....,N \quad (j)$$

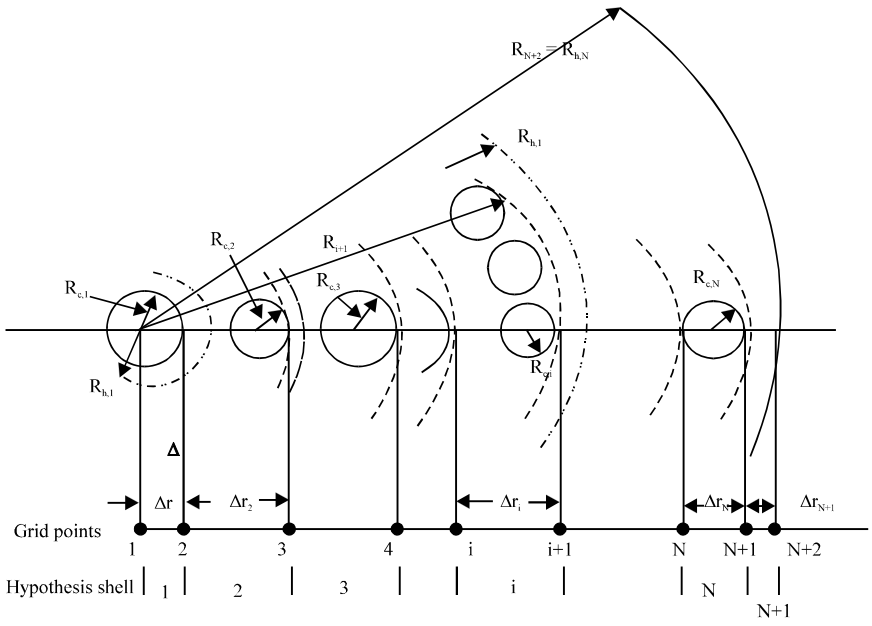


Fig. 2: Catalyst sub particles distribution at time t in the PMGM

$$\text{B.C.2} \quad D_e \frac{\partial M(R_{N+2}, t)}{\partial r} = k_1(M_b - M) \quad (4)$$

where, (M) is the monomer concentration in the macroparticle, ($D_e$) is the effective diffusive of monomer, ($R_p$) is the volumetric rate of polymerization in the macroparticle, $M_b$ is the bulk monomer concentration and ($k_1$) is the film mass transfer coefficient.

Equation 1 is converted to a set of (N+2) Ordinary Differential Equations (ODEs) of monomer concentration at (i) position by using a finite difference technique that was stated by Finlayson (1980), with regard to the unequally spaced grid points as shown in Fig. 2. These equations are list in Table 1. In these, subscript i (i = 1, 2.....N+2), on any variable, indicates its value at the *i*th grid point. The calculations of ($\Delta$r and R) at (ith) position are given in Appendix 1. The radius, ($R_{c,i}$) of the catalyst subparticle in the(ith) shell, are generated randomly using the equations of Nagel *et al*. (1980).

The overall time-dependent reaction rate can be estimated as follow:

$$R_{overall} = \frac{k_p C^* \sum_{i=1}^{N} (N_i M_i)}{\rho_p \sum_{i=1}^{N} N_i} \quad (5)$$

where, $k_p$ is propagation rate constant and C* is the active sites concentration which can be calculated from the kinetic reaction model proposed by Han *et al.* (2007).

Finally, the calculation of polymer properties was carried out by means of the well-known moment technique (Sarkar and Gupta, 1991). The molecular-weight distribution was evaluated by calculating its leading moments, both for living and dead polymer. The nth moment of the chain length distribution of growing polymer in the ith shell is given by a weighted sum of polymer concentrations defined as:

$$\lambda_{pk} = \sum_{n=1}^{\infty} n^k [P_n] \quad (6)$$

Similarly, the moments of the chain length distribution of dead polymer produced by the kth type of site are defined by:

$$\lambda_{Mk} = \sum_{n=1}^{\infty} n^k [M_n] \quad (7)$$

Number-average and weight-average molecular weights are calculated using the following equations:

$$\overline{M_n} = \frac{\lambda_{p1} + \lambda_{M1}}{\lambda_{po} + \lambda_{Mo}} (mw)sty \quad (8)$$

$$\overline{M_w} = \frac{\lambda_{p2} + \lambda_{M2}}{\lambda_{p1} + \lambda_{M1}} (mw)sty \quad (9)$$

where, (mw)sty represents the molecular weight of styrene.

And the Poly Dispersity Index (PDI) is given by:

$$PDI = \frac{\overline{M_w}}{\overline{M_n}} \quad (10)$$

Table 2: Reference values of parameters for simulation

| Parameter | Value | Reference |
|---|---|---|
| $M_o$ (mol $L^{-1}$) | 3.24 | Han *et al.* (2007) |
| C*(mol $L^{-1}$) | $2\times10^{-4}$ | Han *et al.* (2007) |
| $R_o$ (μm) | 20-50 | Han *et al.* (2008) |
| $D_l$ ($cm^2$ $min^{-1}$) | $1\times10^{-8}$ | Schellenberg (2010) |
| $T_o$ (K) | 343 | Schellenberg (2010) |
| $k_d$ ($h^{-1}$) | 1.67 | Han *et al.* (2007) |
| $k_p$ (L $mol^{-1}$ $h^{-1}$) | 8150 | Han *et al.* (2007) |
| Mw (g $mol^{-1}$) | 104.14 | Schellenberg (2010) |

This model was implemented by using Matlab M-Function program and was solved with a sub routine called (ODE15S) which is usually used with stiff differential equations.

A set of reference values of kinetic and physical parameters of syndiotactic polystyrene have been selected and were listed in Table 2.

## RESULTS AND DISCUSSION

The results obtained from this model study the effects of initial catalyst size and initial active site concentration on the rate of polymerization and molecular weight distribution MWD based on a combination features of PGM (Bonini *et al.*, 1995) and PMGM (Sarkar and Gupta, 1991).

In the large particle of high activity catalyst and pores of growing polymer particle, the influence of intraparticle mass transfer will be most pronounced. The mass transfer resistance as a reaction rate will decrease by time; such an increase leads the polymer layer around the catalyst active sites to be thick (Floyd *et al.*, 1986b).

Figure 3 shows steeper monomer concentration profiles as a function of the radial growth of the macro particle at different reaction times. From this figure, it is noticed that the distribution curves of monomer concentration within macro particle growing are present in the first minutes of the reaction. This is because at the beginning of polymerization, the reaction rate is at its maximum while the exposed area of the source monomer is at its minimum.

The effect of the initial catalyst particle size on the particle growth rate is illustrated in Fig. 4 based on the figure; the polymer particle grows to (5-8) times in diameter after (100 min) from initial catalyst. Yet, Fig. 4

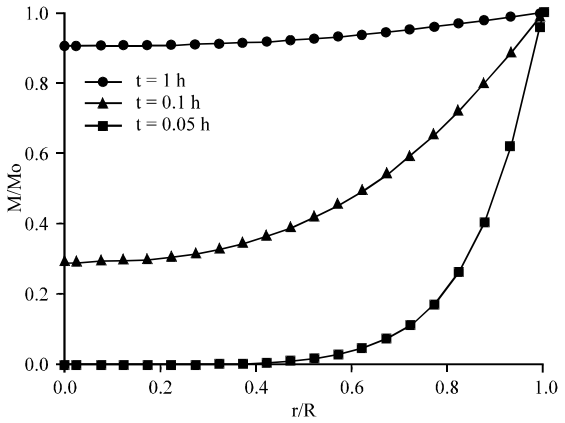


Fig. 3: Profiles of the monomer concentration as a function of radial position at different reaction times

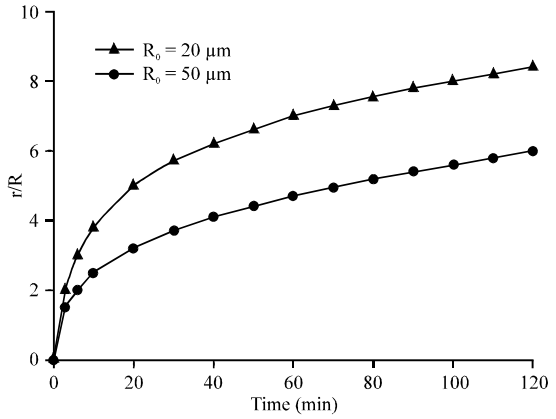


Fig. 4: Particle growth rate with the different initial catalyst size

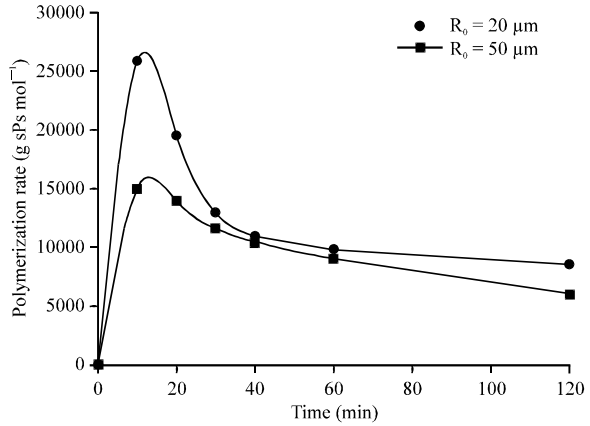


Fig. 5: Effect of initial catalyst size on the rate of polymerization

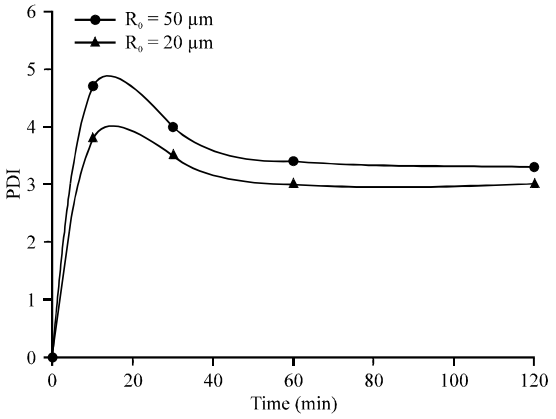


Fig. 6: Polydispersity index over different initial catalyst particle size

also shows that the growing rate of the polymer particle polymerizing from the smaller catalyst particle is faster

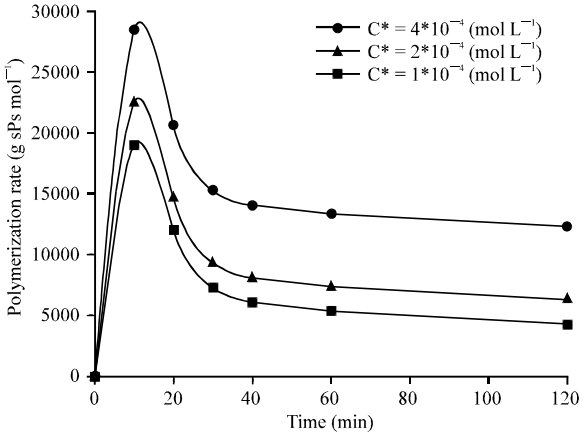


Fig. 7: Effect of catalyst active site concentration on the rate of polymerization

than that from the bigger catalyst particle. In fact, the styrene concentration in the small particles is higher than that in the big particle under the effect of the intraparticle mass transfer resistance. Accordingly, the increase rate of the small particle is faster than that of the big particle via polymerization.

It is beneficial to study the influence of catalyst properties, like that of initial particle size on the dynamic process of particles growth. Figure 5 shows the rates of polymerization at varying initial catalyst size ($R_0$). From this figure, it is illustrated that increasing the size of the catalyst particles leads to a decrease in the rate of polymerization due to the increased rate of the monomer consumption.

The effect of initial catalyst size on PDI illustrated in Fig. 6, it is noticed decreases PDI when the initial catalyst size decrease. The reason why PDI is lower for lower values of initial catalyst size is because of lower diffusional resistance encountered in smaller catalyst particles so to make the difference of monomer concentration between inside and outside of the particle diminish.

On other hand, Fig. 7 depicts the effect of initial catalyst active site concentration (C*) on the polymerization rate, it is observed that the rate of polymerization decreases when (C*) is lowered from $4\times10^{-4}$ to $1\times10^{-4}$ mol L$^{-1}$. A simultaneous lowering of PDI is also observed, as shown in Fig. 8. lowering (C*) lead to two opposite effects: a kinetic effect, i.e., a decrease in the rate of polymerization due to lowering of (C*) itself in the ($k_p$ C* Mi) term and a diffusional resistance leading to higher value of the monomer concentration inside the macroparticle. Obviously, the former effect predominates as far as the rate of polymerization is concerned. Higher monomer

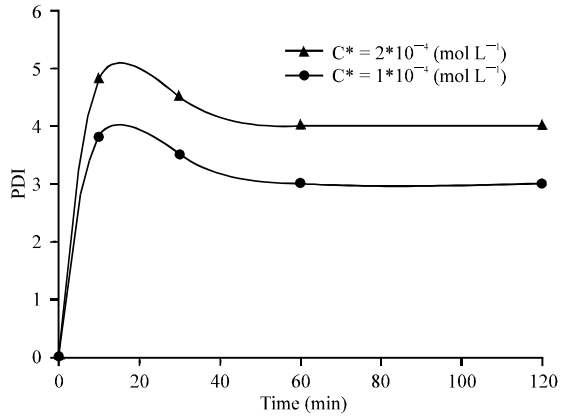


Fig. 8: Polydispersity index over different catalyst active site concentration

concentration inside the macroparticle lead to higher local degree of polymerization (Dp) value since the rate of propagation ($k_p$ C* Mi) has gone up relative to the rate of chain termination. Thus leading to lower PDI.

## CONCLUSION

A comprehensive mathematical model for a single particle growth of syndiotactic polystyrene based on a combination features of the PMGM of Sarkar and Gupta (1992) and PGM of Bonini *et al.* (1995); was developed to predict the effects of initial catalyst size and initial catalyst active site concentration on the rate of polymerization and molecular weight distribution MWD. The simulation results show that a significant distribution of styrene concentration across the radius of polymer particles growth. On other hand, the polymerization rate increase with increasing initial active metal concentration, while changing in the opposite direction under the influence of initial catalyst size. Moreover, the MWD increase with increasing initial active metal concentration and initial catalyst size.

## APPENDIX

The changes in the shells volume, ($\Delta V_i$) and the location of the grid points ($R_i$) with time are given in this section. As shown in Fig. 2. The hypothetical shell can be defined as ($R_{lpi-1} = r = R_{h,i}$) such that the entire polymer produced by the catalyst particles of radius ($R_{c,i}$) are accommodated in it . In the interval (t to t+$\Delta$t), the total volume of polymer and the volume of micro particle produced at ith shell are given by:

$$\frac{dV_i}{dt} = \frac{3.6k_p c^* M_{i+1}\left(N_i \frac{3}{4} R_{c,i}^3\right) mw_{sty}}{\rho c} \quad (11)$$

With $V_i$ (t = 0) being the catalyst and initial pore volume.

$$v_i(t=0) = \frac{N_i\left(\frac{4\pi}{3} R_{c,i}^3\right)}{i-\varepsilon} \quad (12)$$

We can now define the hypothetical shells at any time by:

$$R_{h,i} = \left(\frac{3}{4\pi}\sum_{j=1}^{i} v_j\right)^{1/3} \quad (13)$$

$$R_{h,o} = 0 \quad (14)$$

The catalyst particles are assumed to be placed at the mid points of each hypothetical shell. Thus:

$$R_{1,i} = R_{h,i-1} + \frac{1}{2}\left(R_{h,i} - R_{h,i-1}\right) \quad (15)$$

Then the computational grid points are related to (R1,i) by:

$$R_1\text{-}0 \quad (16)$$

$$R_2 = R_{e,1} \quad (17)$$

$$R_{j+1} = R_{1,i} + R_{e,i} \quad (18)$$

$$R_{N+2}\text{-}R_{h,N} \quad (19)$$

The values of ($\Delta r_i$) to be used in the equation of Table 1 are given by:

$$\Delta_{ri} = R_{i+1} - R_i \quad (20)$$

## ACKNOWLEDGMENTS

The authors would like to thank University Sains Malaysia (USM) for funding this project under Research University Scheme No. (1001/PJKIMIA/811107). The first author gratefully acknowledges the USM for supporting this work under USM Fellowship.

## REFERENCES

Alexiadis, A., C. Andes, D. Ferrari, F. Korber, K. Hauschild, M. Bochmann and G. Fink, 2004. Mathematical modeling of homopolymerization on supported metallocene catalysts. Macromol. Mater. Eng., 289: 457-466.

Bonini, F., V. Fraaije and G. Fink, 1995. Propylene polymerization through supported metallocene/MAO catalysts: Kinetic analysis and modelling. J. Polym. Sci. Part A: Polym. Chem., 33: 2393-2402.

Finlayson, B.A., 1980. Nonlinear Analysis in Chemical Engineering. McGraw-Hill International Book Co., New York, USA., ISBN-13: 9780070209152, Pages: 366.

Floyd, S., K.Y. Choi, T.W. Tylor and W.H. Ray, 1986a. Polymerization of olefins through heterogeneous catalysts. III. Polymer particle modeling with an analysis of intraparticle heat and mass transfer effects. J. Applied Polymer Sci., 32: 2935-2960.

Floyd, S., R .A. Hutchinson and W.H. Ray, 1986b. Polymerization of olefins through heterogeneous catalysis-V. Gas-liquid mass transfer limitations in liquid slurry reactors. J. Applied Polym. Sci., 32: 5451-5479.

Galvan, R. and M. Tirrell, 1986. Molecular weight distribution predictions for heterogeneous Ziegler-Natta polymerization using a two-site model. Chem. Eng. Sci., 41: 2385-2393.

Han, J.J., H.W. Lee, W.J. Yoon and K.Y. Choi, 2007. Rate and molecular weight distribution modeling of syndiospecific styrene polymerization over silica-supported metallocene catalyst. Polymer, 48: 6519-6531.

Han, J.J., W.J. Yoon, H.W. Lee and K.Y. Choi, 2008. Nascent morphology of syndiotactic polystyrene synthesized over silica-supported metallocene catalyst. Polymer, 49: 4141-4149.

Nagel, E.J., V.A. Kirillov and W.H. Ray, 1980. Prediction of molecular weight distributions for high-density polyolefins. Ind. Eng. Chem. Prod. Res. Dev., 19: 372-379.

Sarkar, P. and S.K. Gupta, 1991. Modelling of propylene polymerization in an isothermal slurry reactor. Polymer, 32: 2842-2852.

Sarkar, P. and S.K. Gupta, 1992. Simulation of propylene polymerization: An efficient algorithm. Polymer, 33: 1477-1485.

Schellenberg, J., 2009. Syndiotactic Polystyrene: Synthesis, Characterization, Processing and Applications. John Wiley and Sons Inc., Nerw York, USA., ISBN-13: 9780470286883, Pages: 484.

Schellenberg, J., 2010. Syndiotactic Polystyrene: Synthesis, Characterization, Processing and Applications. John Wiley and Sons Inc., Hoboken, NJ., USA.

Singh, D. and R.P. Merrill, 1971. Molecular weight distribution of polyethylene produced by Ziegler-Natta catalysts. Macromolecules, 4: 599-604.